Construction and Building Materials 323 (2022) 126559

Contents lists available at ScienceDirect

Construction and Building Materials

journal homepage: www.elsevier.com/locate/conbuildmat

Short-term resilient behaviour and its evolution with curing in cold in-place recycled asphalt mixtures

P. Orosa *, I. Pérez, A.R. Pasandín

Universidade da Coruña, Department of Civil Engineering, E. T. S. I. Caminos, Canales y Puertos, Campus de Elviña s/n, 15071, A Coruña, Spain

ARTICLE INFO

Keywords:
Cold in-place recycling (CIR)
Reclaimed asphalt pavement (RAP)
Bitumen emulsion
Asphalt mixture
Triaxial testing
Gyratory compactor
Nonlinear elastic behaviour
Resilient modulus
Resilient behaviour

ABSTRACT

This study evaluates the short-term resilient behaviour of cold in-place recycled (CIR) asphalt mixtures with bitumen emulsion when they are more similar to non-cohesive granular materials than to conventional hot mixtures. Gyratory compacted CIR specimens were manufactured using different proportions of bituminous emulsion and water, and dynamic triaxial tests were conducted at different curing times. The resilient moduli were obtained experimentally and fitted using three numerical models. Characteristic nonlinear elastic behaviour and an increase in stiffness with curing time were observed. Water loss during curing and stiffness increase were found to be related. Mixtures with 2.50% residual bitumen and 2.75% added water showed the best short-term stiffness evolution.

1. Introduction

With the limited service life of pavement, the maintenance and repair of road networks is a major concern. Cold in-place recycling (CIR) with bitumen emulsion is a preferred method for pavement rehabilitation [1]. CIR has unique advantages over other maintenance and rehabilitation treatments, with environmental benefits [1–7] including the reduction of greenhouse gas emissions, owing to the preservation of materials and the use of cold techniques. In addition, pavement recycling reduces costs by reducing energy consumption and the need for material transport [8], and by reusing materials on site, achieving cost savings of up to 50% compared to conventional rehabilitation techniques [9].

The main constituents of a CIR asphalt mixture are recycled aggregate known as reclaimed asphalt pavement (RAP), obtained from the milling of worn roads, a bituminous binder acting as a stabiliser in the mix, generally used in the form of emulsion or foamed bitumen, and a certain amount of added water to facilitate the blending process and ensure the proper moisture content [10]. The addition of virgin aggregates (for gradation adjustment) or fillers to improve the mechanical properties of the mixture, including fly ash and Portland cement, are also commonly considered [11–14]. Unlike traditional hot asphalt mixtures, no heating is required in the manufacturing process, and water is an essential component in the mixtures. Some of the water is expelled during compaction; the remainder evaporates slowly over time during the curing period. In addition, when Portland cement is added to the mixtures, part of the added water is involved in the hydration process [10,13–15].

These recycled mixtures, also known as bitumen-stabilized materials (BSMs) [16,17], combine the distinctive characteristics of their components. They are characterised by great flexibility, reduced stiffness, and lower susceptibility to shrinkage cracking because the binder in BSMs is diffused among the fine aggregates, creating local links between the skeleton of the coarse aggregates [16,17]. Jenkins et al. [18] and Ebels [19] concluded that after the preparation of such mixtures, there are two distinct phases in their mechanical behaviour. The curing phase is characterised by an increase in early resistance capacity and stiffness owing to moisture reduction, followed by a second phase of stiffness reduction caused by aging and traffic loads. The same authors also indicated that during the first phase, nonlinear elastic behaviour is evident (resembling that of granular materials, characterised by stress dependence [20]); in the second phase, the behaviour is viscoelastic (similar to that of an HMA, characterised by temperature and loading frequency dependence [21,22]). Authors such as Casillas et al. [23] suggested naming "semi-bound" materials to the ones that present characteristics of non-cohesive granular materials and HMA, but behave differently during the curing period. Thus, it is considered essential to study the evolution of the properties (workability, compactability, and

* Corresponding author.
E-mail addresses: p.orosa@udc.es (P. Orosa), iperez@udc.es (I. Pérez), arodriguezpa@udc.es (A.R. Pasandín).

https://doi.org/10.1016/j.conbuildmat.2022.126559
Received 26 April 2021; Received in revised form 13 September 2021; Accepted 20 January 2022
Available online 31 January 2022

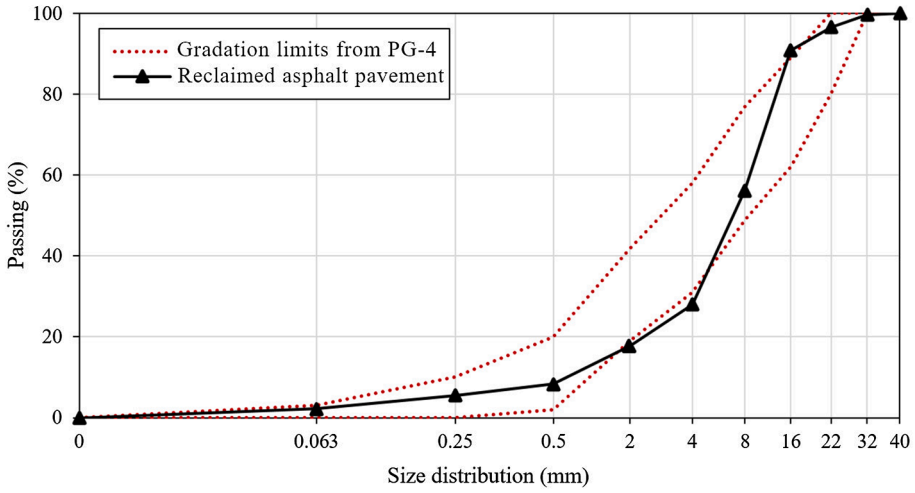

Fig. 1. RAP gradation compared with limits in PG-4 specification.

cohesion gain) during this period, and not only the final performance of the cured material.

Despite numerous studies examining the curing of cold recycled mixtures, the process is not fully understood, nor are the time required and the phenomena that occur. Studies have concluded that 28 d was sufficient time for a cold mixture to evaporate almost all of its water content [15]. However, the curing process also involves mechanisms that lead to an increase in the stiffness and strength of the mixtures, which last longer. Other studies on CIR mixtures have reported a curing time from 6 to 18 months, during which the stiffness continues to increase [24–26]. There is no consensus; thus, a better understanding of the curing mechanism and early strength evolution of CIR mixtures is essential. This knowledge would contribute to the development of standardised curing procedures, both in the laboratory and in situ, allowing better estimation of the time required before opening to traffic.

For this purpose, the evolution of the stiffness of different CIR mixtures during the curing period was investigated in laboratory conditions in this study. The resilient modulus (M_r), understood as the discharge modulus value measured after a large number of loading cycles, is widely accepted in road design as a suitable measure of pavement course stiffness. Thus, based on the mechanical behaviour of cold recycled mixtures during the curing phase, triaxial tests were conducted under cyclic stress with a constant confining pressure, applying specific assumptions for tests performed on granular materials without binder [21,27–29].

2. Aims and scope

This study was motivated by a need to understand the mechanical behaviour of CIR mixtures, particularly in the short term, and its evolution in the curing period.

Because different proportions of CIR constituents affect the mechanical characteristics, different dosages were used to study CIR stiffness in more depth. To this end, CIR mixtures were manufactured with residual binder proportions varying from 1.50% to 3.50%, and added water varying from 0.25% to 3.75% (depending on the residual binder content). The contents of added water were estimated using equations from two different Spanish specifications, in order to determine which is the most suitable for CIR based on the results of the stiffness evolution. A bituminous emulsion was used as binder; the use of additives was not considered. Dynamic triaxial tests were performed to obtain the resilient moduli at different curing times. The specimens were tested several hours after fabrication in laboratory conditions, and after multiple days of curing.

The main objective was to evaluate the influence of different dosages on the developed stiffness, and to assess its evolution with ageing. Additionally, three prediction models were adjusted to the obtained results, which could be used for numerical simulation of the behaviour of the mixtures.

3. Materials and manufacturing

3.1. RAP

The RAP was supplied by a local contractor from the milling of surface pavement courses. Its size gradation is shown in Fig. 1, compared with the gradation limits established in the Spanish PG-4 specification [30] for recycled pavements. The properties of the RAP and its recovered binder are presented in Table 1.

In Fig. 1, and compared to RAP gradations from other CIR studies [14], the RAP has a high content of coarse particles and aged binder. The high recovered binder content is attributed to the crushing of surface courses, which usually have the highest bitumen content. The Spanish PG-4 specification for CIR mixtures [30] does not limit the use of RAP in terms of the presented characteristics. Furthermore, despite not exactly fitting the PG-4 limits, no grain size corrections were made to investigate

Table 1
Properties of RAP, recovered binder, and residual binder of bitumen emulsion.

Property	Standard	Result	
RAP bulk density (kg/m3)	EN 1097–6 [31]	2560.00	
RAP recovered binder content (%)	NLT-164/90 [32]	7.81	
		RAP recovered binder	Emulsion residual binder
Softening point (°C)	EN 1426 [33]	64.40	36.50
Penetration (10^{-1} mm)	EN 1427 [34]	20.32	170.00

Table 2
AWC estimation according to PG-4 specifications.

Specification:	AWC estimation:	
Circular Order 8/2001 [38]	% AWC = % OFC – 0.5% – % EC	Eq. (1)
Circular Order 40/2017 [30]	% AWC = % OFC – 0.5% – % BC	Eq. (2)

Table 3
Residual binder, bitumen emulsion, and added water contents.

		AWC (%)						
BC (%)	EC (%)	Eq. (1)	Eq. (2)	Additional contents				
1.50	2.50	2.75	3.75					
2.00	3.33	1.92	3.25					
2.50	4.17	1.08	2.75	1.50	2.00	2.50	3.00	3.50
3.00	5.00	0.25	2.25					
3.50	5.83		1.75					

as closely as possible what actually happens in the CIR, as it was already done in previous reported cases [35,36]. Hence, this investigation is a continuation of the study of their behaviour.

3.2. Bitumen emulsion

A slow-setting cationic emulsion with 60% bitumen content (BC) was used in this study. In accordance with EN 13,808 [37], it was a C60B5 REC bitumen emulsion. A national hydrocarbon company provided the bitumen emulsion for this study, with the same characteristics reported in previous studies on CIR mixtures [35,36]. Table 1 present the softening point and penetration results of the residual bitumen used to produce the bituminous emulsion.

3.3. Specimen preparation

Residual bitumen and added water contents

To study the resilient behaviour, CIR specimens were prepared with 100% RAP, with different amounts of bitumen emulsion (EC) and added water (AWC). Fourteen dosages were used; in each case, three specimens were prepared (resulting in 42 total specimens). As done in previous studies for these mixtures [35], the recommendations in the PG-4 specifications for recycled mixtures from 2001 [38] and 2017 [30] were followed for calculation of the AWC. This calculation aims to maintain the optimum fluid content (OFC) of the mixtures using Eqs. (1) and (2) shown in Table 2, depending on the result of the modified Proctor test (MPT) and the amount of binder used in each case.

The RAP was the same as that used in a previous study [35,36], with an MPT result of 5.75%. This value was used as the OFC in Eqs. (1) and (2) for all mixtures. Thus, the BC ranged from 1.50 to 3.50%; 1.50% is the minimum indicated in the PG-4 specification [30] for CIR mixtures, and 3.50% is the maximum content to maintain the OFC according to Eqs. (1) and (2). For the BC that produced the highest resilient moduli in the mixtures, five more AWC were considered. The 14 mixtures are summarised in Table 3.

The BC and AWC for each group were used to identify them (the group of specimens with 2.00% BC and 1.92% AWC was denoted as "2B_1.92 W").

Mixing and compaction procedures

The same mixing process was used as in previous studies [35,36], by using an automatic asphalt mixer. The RAP and AWC were mixed for 60 s; the EC was added to the mixture and mixed for 90 s, for a total blending time of 150 s. This procedure was based on recommendations and previous laboratory experience with this type of mixture [35,36,39].

Once the mixing was completed, the samples were extracted from the mixer and placed in the mould of the gyratory compactor. Based on the PG-4 specifications for CIR mixtures [30], gyratory compaction was used with 100 gyrations and 100 mm diameter moulds, according to EN 12697–31 [40]. The moulds used present horizontal holes which allow water drainage if necessary. This type of mould proved to be the most suitable for cold mixtures according to previous studies on compaction carried out by Orosa et al. [36]. The compactor parameters included an internal rotation angle of 0.82°, a rotation speed of 30 rpm, and a compaction pressure of 600 kPa [40]. According to EN 13286–7 [41], the height of the triaxial specimens must be twice their diameter. Accordingly, specimens were manufactured by piling two compacted specimens with a height and diameter of 100 mm, resulting in specimens 200 mm in height.

Specimens compacted with the gyratory compactor were sufficiently stable to allow extrusion and stacking immediately after compaction. Once the specimens were stacked one on top of the other the curing time

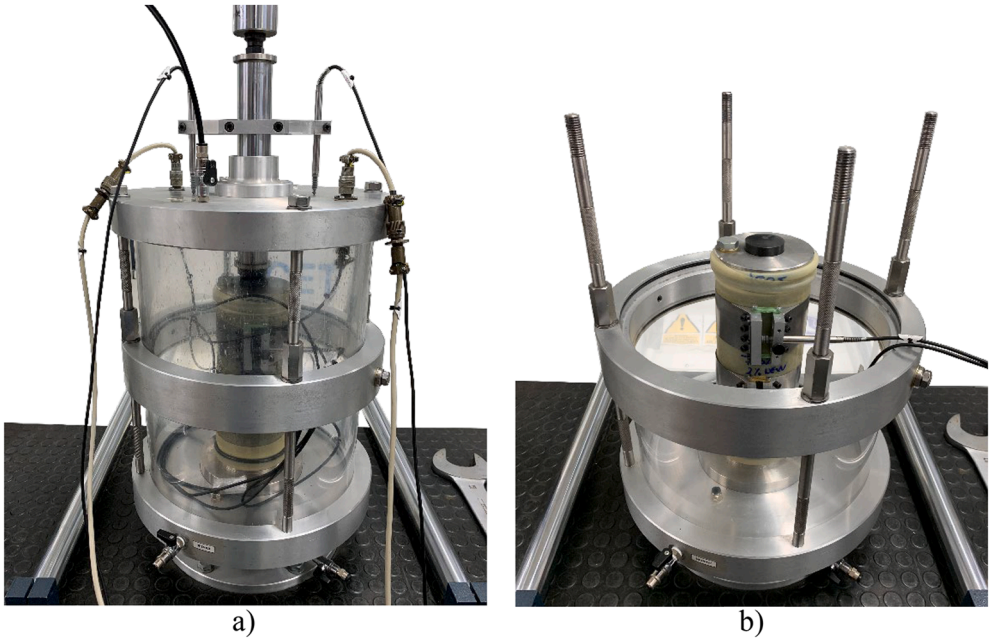

Fig. 2. Positioning of specimen and strain sensors for triaxial test (EN 13286–7): a) open triaxial chamber; b) closed triaxial chamber.

Table 4
Stress levels in sequences of resilient modulus test (EN 13286–7).

Sequence	Confining pressure, σ_3 (kPa)	High deviator stress, σ_d (kPa)	Low deviator stress, σ_d (kPa)
1	20	30	20
2		50	35
3		80	50
4		115	70
5	35	50	35
6		80	50
7		115	70
8		150	90
9		200	120
10	50	80	50
11		115	70
12		150	90
13		200	120
14		280	160
15	70	115	70
16		150	90
17		200	120
18		280	160
19		340	200
20	100	150	90
21		200	120
22		280	160
23		340	200
24		400	240
25	150	200	120
26		280	160
27		340	200
28		400	240
29		475	300

started. This fabrication procedure has been used in previous studies [20,26,38,39], with the same behaviour as a single specimen in compression tests, with stresses applied on the main axis of the specimen.

Moisture evolution and curing procedure

All specimens were air-cured in the laboratory, within a controlled conditions environment (temperature of 22 ± 2 °C and relative humidity of 50 ± 5%). All tests were repeated for specimens at different curing ages to evaluate the effect of air curing on the results. With curing time, the specimens gradually lose water by evaporation and their weight decreases. Graziani et al. [15] concluded that 28 d was enough time for a cold recycled mixture to evaporate almost all its water content. However, for confirmation, given the particularity of each mixture, seven triaxial-size specimens with different dosages of BC and AWC were manufactured and maintained in laboratory conditions. BCs of 1.50%, 2.00%, 2.50%, 3.00%, and 3.50% were used, with AWCs resulting from Eqs. (1) and (2), and showed in Table 3. The specimen weights were periodically measured during the time necessary to reach a constant weight. Weight measurements were recorded at 0 d, 1 d, 3 d, 7 d, 15 d, 30 d, 60 d, and 180 d, and were considered "constant weight" when the difference in weight from one to the next was less than 0.01%.

Supported by the additional assessment of the moisture evolution of the specimens with curing time at room conditions, five air-curing ages were considered. The first triaxial tests were performed on "uncured" specimens, 4 h after manufacture (0 d). After 3d, 7 d, 30 d, and 60 d, the tests were repeated on the same specimens, to determine the evolution of the CIR mixture stiffness with air curing.

4. Resilient behaviour of CIR mixtures

4.1. Dynamic triaxial testing

The resilient moduli of the mixtures were obtained through dynamic triaxial tests on the manufactured CIR specimens. The experimental equipment for these tests consisted of an extractable chamber and a device to generate an axial load (Fig. 2). A confining pressure was applied inside the chamber (up to 10 bar) using an air compressor. A hydraulic system, independent of the previous one, managed the axial load.

For effective confinement of the specimens using the pneumatic system, the specimens were isolated inside an enclosed elastic membrane attached to the upper and lower porous plates by O-rings to avoid pressurised air from penetrating the membrane.

The axial deformations were recorded using two linear variable strain transducers (LVDTs) installed on the top plate of the chamber (Fig. 2a).

A constant confining pressure (CCP) was applied with a sinusoidal deviator strain, as indicated in EN 13286–7 [41]. According to the standard [41], two stress levels can be applied to the tested specimen (low and high levels) to better simulate the stresses that pavement layers are subjected to during their service life. These applied stresses correspond to those normally present in the upper part of the base course, under a thin bituminous wearing course (less than 80 mm).

The test begins with a conditioning phase involving a constant confinement of 70 kPa (σ_3) combined with a cyclic axial deviator stress (σ_d) ranging from 5 to 340 kPa for the high stress level, and from 5 to 200 kPa for the low stress level, at a frequency of 1 Hz (0 kPa stress is avoided to guarantee constant specimen contact with the actuator). The conditioning was considered complete when at least one of the following requirements was met:

- The permanent axial strain rate was less than 10^{-7} per cycle.
- The resilient modulus variation rate was less than 5 kPa per cycle.
- The number of cyclic deviator stresses was greater than 20,000 cycles.

When the conditioning phase was completed, the resilient modulus test began; 29 loading sequences were conducted with different σ_3 and σ_d combinations, depending on the stress level (Table 4); σ_3 remained fixed in each sequence, with a cyclic variation of σ_d. One hundred loading cycles per sequence were performed at 1 Hz frequency. The resilient modulus M_r was calculated as the average result of the moduli of the last ten cycles for each sequence, expressed as

$$M_r = \sigma_d/\varepsilon_r \quad (3)$$

where σ_d is the amplitude of the deviator stress and ε_r is the resilient elastic deformation.

The high stress level was used in all cases, except in the triaxial tests conducted at 0 d of curing, when the specimens had not yet developed sufficient stiffness and were considered more sensitive.

For each mix, three specimens were tested. The triaxial tests were conducted 4 h after manufacture (0 d), after which the specimens continued curing; tests were conducted again at 3d, 7 d, 30 d, and 60 d. Specimens were handled carefully during the entire process, preventing any damage during instrumentation or curing. For each group of three identical specimens, the average result of the tests at each curing age was calculated to assess the evolution of M_r and compare the results between the different mixes.

4.2. Computational modelling of resilient behaviour

Many nonlinear models have been proposed to reproduce the performance of unbound aggregates and coarse-grained soils [20,42–45]. In this study, once the experimental results were obtained from dynamic triaxial tests, three models were used to estimate the M_r of the CIR mixtures with different air curing times.

The first model is known as the k-θ model, proposed by Hicks [46]. This model describes the resilient modulus in terms of the sum of principal stresses (the first stress invariant, $\theta = \sigma_1 + 2\sigma_3$):

$$M_r = k_1 \cdot \theta^{k_2} \quad (4)$$

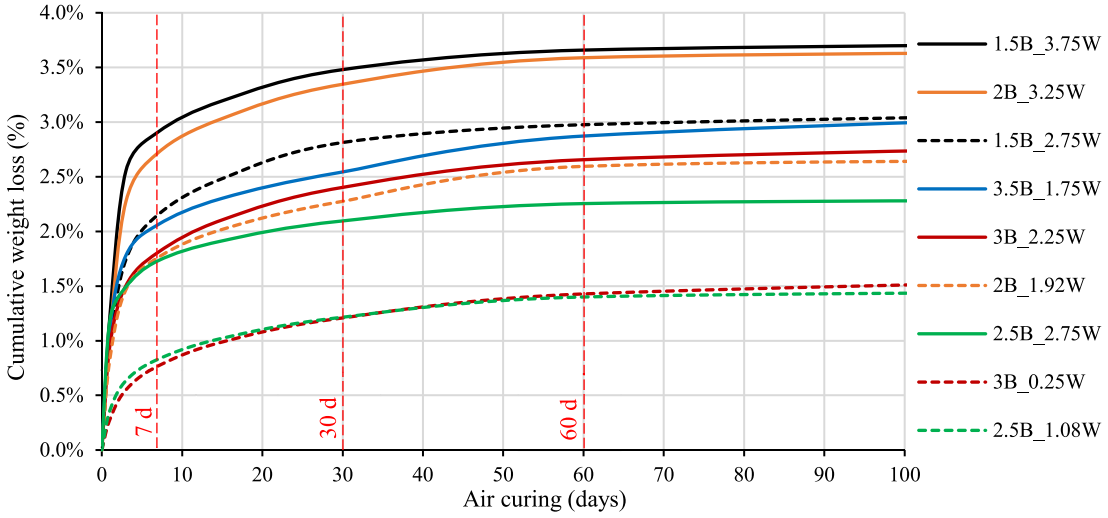

Fig. 3. Weight loss of CIR specimens over time with air curing.

where k_1 and k_2 are material constants. A major feature of the k-θ model is its inherent simplicity; it considers that the variation in the elastic response is exclusively a function of the principal stresses and neglects the effect of shear stress. It is still the most widely used and accepted mathematical relationship for unbound aggregates.

Nevertheless, the model oversimplifies the stress dependence in many cases, as most resilient moduli of pavements and unbound material are dependent on the bulk stress and the shear strain magnitude. In asphalt mixtures, interparticular forces are produced by a bituminous binder that gives the material a certain degree of cohesion, which motivated Uzan et al. [47] to consider the effect of the deviator stress (σ_d), expressed as

$$M_r = k_1 \cdot \theta^{k_2} \cdot \sigma_d^{k_3} \tag{5}$$

New models have been developed that consider the variation in the Poisson's ratio with stress level, or the influence of the density of the material. The Mechanistic-Empirical Pavement Design Guide (MEPDG) uses a modified version of Uzan's equation, which was advocated by the National Cooperative Highway Research Program (NCHRP) [48] in 2004, and is considered in this study.

$$\frac{M_r}{P_a} = k_1 \left(\frac{\theta}{P_a}\right)^{k_2} \left(\frac{\tau_{oct}}{P_a} + 1\right)^{k_3} \tag{6}$$

$$\tau_{oct} = \frac{1}{3}\sqrt{(\sigma_1 - \sigma_2)^2 + (\sigma_1 - \sigma_3)^2 + (\sigma_2 - \sigma_3)^2} = \frac{\sqrt{2}}{3}\sigma_d \tag{7}$$

where the octahedral stress, τ_{oct} , replaces the deviator stress, and Pa is the reference pressure (101.35 kPa); k_1, k_2, and k_3, are inherent constants of the material. The NCHRP model is a simplified version of a more complex model developed by Andrei [49] that included seven material constants.

All parameters in the proposed models were determined using the optimisation solver function in Excel, minimising the quadratic error between the model values and the actual modulus values obtained experimentally in the laboratory. The predictive model parameters are a useful tool, and can be used to perform numerical simulations of the behaviour of CIR mixtures in future research.

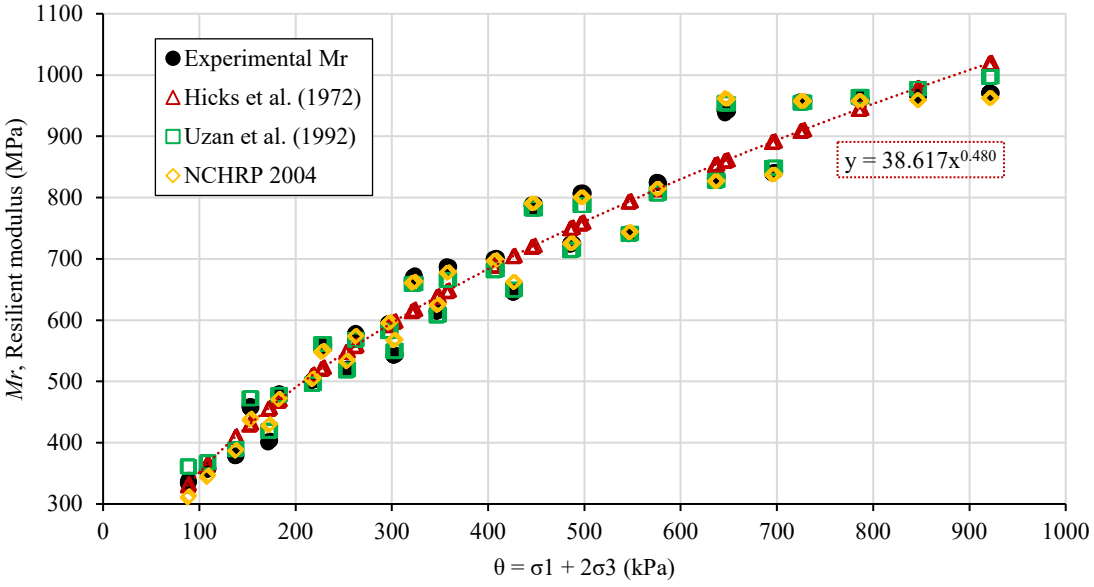

Fig. 4. Experimental results of M_r and fitted computational models of CIR mixture 2B_1.92 W at 7 d of curing.

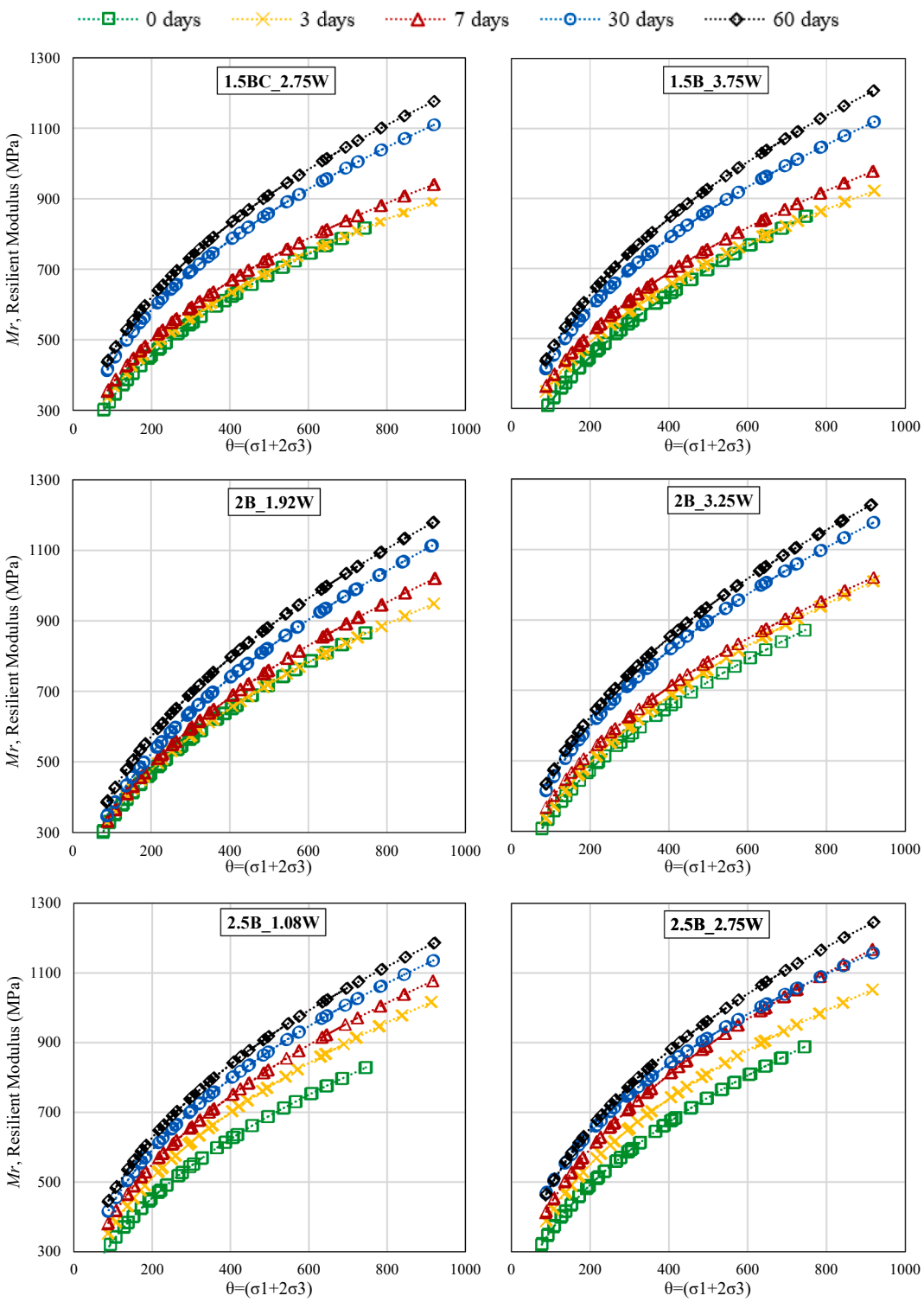

Fig. 5. Representation of the fitted Hicks model for the CIR mixtures designed according to PG-4 specifications, at 0 d, 3 d, 7 d, 30 d, and 60 d of curing time.

5. Results

5.1. Moisture evolution at room temperature

In addition to the results reported from previous studies, the weight loss of specimens manufactured with all the BC considered, and the AWCs resulting from Eqs. (1) and (2) were recorded over time to assist in the choice of curing times. Fig. 3 shows the cumulative percentage of weight loss in the specimens due to water evaporation.

The graph in Fig. 3 shows that weight losses increased rapidly during the first week after manufacturing due to a greater water content at that time, leading to faster evaporation. From 7 d to 30 d, and more noticeable from 30 d to 60 d of curing, the weight gradually stabilized. After air curing for 60 d, the weight was considered constant according to the established criteria.

Vertical separation due to the total AWC in the mixtures was

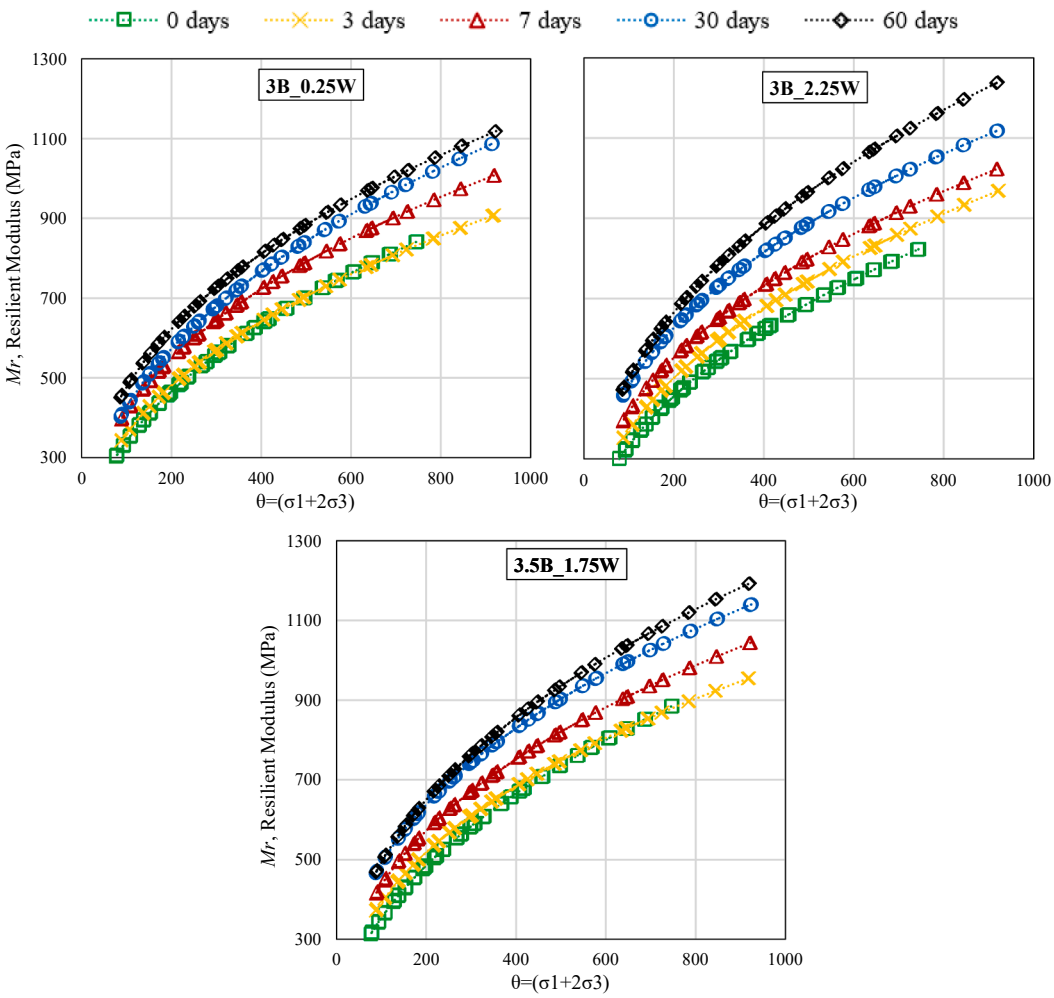

Fig. 5. (*continued*).

observed; the curves at the top represent a higher weight loss (water loss) as a result of a higher initial amount of water in them that could be evaporated. Thus, these mixtures with higher initial fluid content also showed a faster rate of weight loss in the first days (as shown by the different slopes of the curves during the first week of curing). As curing progressed, the remaining water to evaporate decreased and the curves in Fig. 3 became more parallel, stabilizing their evaporation rate. Thus, in view of the significant water losses in the first days, the mechanical behaviour was analysed by performing triaxial tests at 0 d, 3 d, and 7 d. Subsequently, the tests were also repeated at 30 d and 60 d, thereby determining the influence of water loss on the evolution of the stiffness of the CIR mixtures, both in the short term and for more advanced curing periods.

5.2. Resilient behaviour of CIR mixtures

5.2.1. Dynamic triaxial testing

After curing and the conditioning phase were completed, triaxial tests were conducted according to the load sequences in Table 4.

With the six confining pressures (σ_3) used during the test, the resilient modulus results were collected in six ''steps''. As expected, M_r increased from step to step, but also increased within each step, although at a slower rate, with an increase in the deviatoric stress (σ_d). The increase in M_r with increasing stress reveals the nonlinear behaviour of CIR mixtures, similar to that of unbound granular materials. As an example, the graph in Fig. 4 shows the average result of the triaxial tests for group 2B_1.92 W after 7 d of curing. The adjusted numerical models are plotted in the same figure for comparison. The step shape is observed in the experimental results, and in the Uzan and NCHRP models, which accurately predicted the actual results, with an average R^2 of 0.9963 and 0.9939, respectively. The Hicks model is simpler, approximating the result by means of a potential function without reproducing the steps, showing an average R^2 of 0.9578, and therefore approximating the *Mr* not as closely as the two previous models.

The simplicity of the Hicks model allows better visual comparison between mixtures and curing times than the models with step shapes. Thus, the graphs in Fig. 5 show the evolution of *Mr* results obtained using the fitted Hicks model at the different curing times for the mixtures that used the AWC specified in PG-4 [30,38], to meet the OFC specifications. In addition, Table 5 summarizes the ranges of experimental results of *Mr* obtained in the triaxial test for all the studied mixtures, at the considered curing times. This table allows a simple comparison of the maximum *Mr* values obtained by different mixtures for a given curing time, as well as to monitor the evolution of the *Mr* results for a certain mixture.

In Fig. 3, most of the water evaporated in the first days after production, and the evaporation rate decreased after 7 d. This fact may explain why in both Fig. 5 and Table 5 the main differences in the behaviour of the mixtures were observed during the first few days of curing, in the results corresponding to 0 d, 3 d, and 7 d, showing greater increases in *Mr* than for more advanced curing times. For example, in mixture 2B_1.92 W, the percentage increase in the maximum M_r value between 0 d and 7 d was 17.06% (i.e., 2.44% per day), 10.10% between 7 d and 30 d (i.e., 0.44% per day), and 6.50% between 30 d and 60 d (i.

Table 5
Resilient modulus (M_r) ranges for different curing times.

Mixture	M_r range (MPa) for different curing times				
	0 d	3 d	7 d	30 d	60 d
1.5B_2.75 W	296.23 to 789.99	346.37 to 861.99	365.85 to 908.81	418.33 to 1080.88	443.43 to 1145.73
1.5B_3.75 W	284.02 to 805.33	366.05 to 882.71	381.94 to 941.55	423.85 to 1077.58	446.45 to 1173.13
2B_1.92 W	307.94 to 830.51	321.51 to 902.86	334.38 to 972.22	355.29 to 1070.40	385.22 to 1140.00
2B_3.25 W	295.99 to 830.61	332.87 to 957.60	357.64 to 973.01	418.21 to 1141.90	450.63 to 1200.84
2.5B_1.08 W	295.54 to 791.42	346.84 to 974.20	392.03 to 1032.24	429.87 to 1107.10	466.77 to 1163.68
2.5B_1.5 W	324.23 to 827.05	374.52 to 948.06	398.65 to 1018.66	439.54 to 1117.96	466.38 to 1202.58
2.5B_2W	354.51 to 882.09	382.14 to 1026.13	433.43 to 1049.93	424.35 to 1145.05	462.55 to 1212.39
2.5B_2.5 W	330.81 to 865.54	374.40 to 1028.57	444.33 to 1057.43	472.12 to 1135.88	465.36 to 1202.44
2.5B_2.75 W	318.60 to 868.85	367.56 to 1029.59	412.19 to 1117.11	456.89 to 1134.99	472.64 to 1216.72
2.5B_3W	325.38 to 877.68	402.18 to 1007.12	403.12 to 1059.84	440.92 to 1088.72	476.37 to 1212.74
2.5B_3.5 W	280.78 to 786.97	342.59 to 911.04	403.98 to 1001.90	482.47 to 1100.15	505.35 to 1281.33
3B_0.25 W	298.64 to 804.81	340.52 to 869.00	407.86 to 974.42	463.15 to 1080.26	426.77 to 1060.06
3B_2.25 W	303.70 to 792.66	350.41 to 918.52	390.68 to 975.61	487.04 to 1100.83	478.11 to 1187.90
3.5B_1.75 W	313.39 to 878.41	374.81 to 917.77	422.64 to 1003.15	481.54 to 1116.10	495.79 to 1168.56

e., 0.22% per day). Thereby implying a relationship between the increases in stiffness with the rate of water evaporation in the samples with curing time. The increasing trend of M_r was generally observed in all mixtures (Table 5). The M_r values were found to be consistent with results reported in other studies for similar cold recycled mixtures [19,21,26,28,49–51].

Considering the results at 0 d shown in Table 5 and Fig. 5, the results are similar between groups, as the binder influence is minimal at this point; the behaviour of CIR mixtures at 0 d resembles that of an unbound granular material, resisting loads mainly through its mineral structure. From Table 5, the difference between the maximum and minimum values of the upper limits of the ranges reached 95.11 MPa. However, it is worth noting a tendency towards higher *Mr* values in mixtures with higher BC. As the curing time progressed, the dispersion of *Mr* results in Table 5 increased, showing an increased influence of the different BC and AWC dosages. At 60 d of curing, the difference between the maximum and minimum values of the upper limits of the ranges reached 221.26 MPa, more than twice the difference for the uncured specimens.

Concerning the BC, the graphs in Fig. 5 showed that as the BC of the mixtures increased, their *Mr* results reached higher values in the short term. Mixtures with 1.50% BC had the lowest *Mr* results in all the short-term triaxial tests performed, with an increase between the maximum *Mr* values reached at 0 d and at 7 d of 15–17%. Mixtures that increased the amount of BC showed a better evolution of the *Mr*, being the mixtures with 2.50% BC the ones that had the highest *Mr* values as well as the best evolution, with an increase of 28–30% between the results achieved at 0 d and at 7 d. The mixtures with the highest BC (i.e., 3.00% and 3.50% BC) also showed better results than those obtained in mixtures with 1.50% BC, but worsened compared to those obtained with 2.50% BC. For these mixtures the highest BC, *Mr* values increased between 0 d and 7 d by 21–23% for mixtures using 3.00% BC, and by 14% for those using 3.5% BC. It is concluded that the 2.50% BC is the optimum content in terms of the short-term evolution of the Mr, as well as for the maximum values obtained.

Considering the evolution of the *Mr* results in Fig. 5 at 30 d and 60 d, all mixtures exceeded 1000 MPa at 30 d, and 1100 MPa at 60 d. However, the results obtained in the mixtures with 2.50% BC were again the highest, presenting maximum values of *Mr* about 3–5% higher than the average of the studied mixtures even for longer curing times (Table 5).

Regarding the amount of water used in the mixtures represented in Fig. 5, those with higher AWC, and designed based on Eq. (2, presented in all cases higher *Mr* results and faster evolution than those with the same BC and lower AWC (designed based on Eq. (1)). It could be observed from the values in Table 5, for example, that at 7 d of curing the maximum *Mr* value obtained by the mixture 2.5B_2.75 W was 8.22% higher than that obtained by 2.5B_1.08 W. This highlighted the important role of water in mix design, improving mixing and compaction processes, enhancing both short and long-term performance. Thus, the mixture with the lowest AWC of all the studied mixtures (3B_0.25 W), despite having a high binder content, ended up presenting some of the lowest *Mr* results due to the lack of an adequate AWC dosage, even showing a 2.60% reduction of the maximum *Mr* between 30d and 60d of curing.

As already mentioned, it was found that the water loss of the specimens during the curing process was closely related to the evolution of the *Mr* results obtained. The graphs in Fig. 6 show this correlation In each plot, mixtures with the same BC and the considered AWCs were represented. Each marker corresponds to a curing time (0 d, 3 d, 7 d, 30 d, and 60 d). The vertical axis represents the average of the maximum *Mr* achieved in the triaxial tests for the maximum stress condition by the three tested specimens of each mixture (i.e., the upper limit of the *Mr* ranges in Table 5). The horizontal axis represents the cumulative water loss of the specimens during the curing time, expressed as a percentage of the initial weight of the specimens.

The relationship shown in the graphs in Fig. 6 proved to be reasonably linear, especially for the intermediate BC used (2.00%, 2.50%, and 3.00% BC). It was detected that mixtures that used a minor AWC in their design, and consequently had a lower percentage of water loss, reached lower maximum *Mr* values than the mixtures with the same BC and a higher AWC.

Therefore, it was concluded that for the CIR mixtures studied in this research, the optimum BC in terms of resilient behaviour was 2.50% BC; in a previous study [35], 2.50% BC was also found to be the optimum binder content. In the mixtures initially studied with 2.50% BC, the AWC was a critical factor for the obtained *Mr* values and evolution. Thus, five additional mixtures were studied by varying the AWC. The graphs in Fig. 7 show the evolution of the *Mr* with the curing time of all the mixtures manufactured with 2.50% BC, fitting the Hicks model to the experimental results.

The graphs in Fig. 7 showed that the dispersions were greater in the results at 0 d and 3 d. Considering the values in Table 5, it can be seen that the variation between the maximum and the minimum of the upper limits of the *Mr* ranges obtained for the mixtures with 2.50% BC was 132.45 MPa and 118.55 MPa, respectively. In both curing cases, mixtures using the highest and the lowest AWCs (1.08%, 1.50%, and 3.50% AWC) showed the lowest M_r, again revealing the important role of water in the right proportion on the mix design. For mixtures using the "intermediate" AWCs (2.00%, 2.50%, 2.75%, and 3.00% AWC), the results were higher and more homogenous, being at 3 d the difference between the maximum and the minimum upper limits of *Mr* ranges reached 22.47 MPa.

In the graph corresponding to the 7 days of curing in Fig. 7, the *Mr* reached by the mixture with 2.75% AWC (designed using Eq. (2 from CO 8/2017 [30]) stood out from the rest. This mixture also presented the best evolution in the graphs of Fig. 5, reaching *Mr* values at 7 d very close to those obtained at 30 d for the higher stress levels considered.

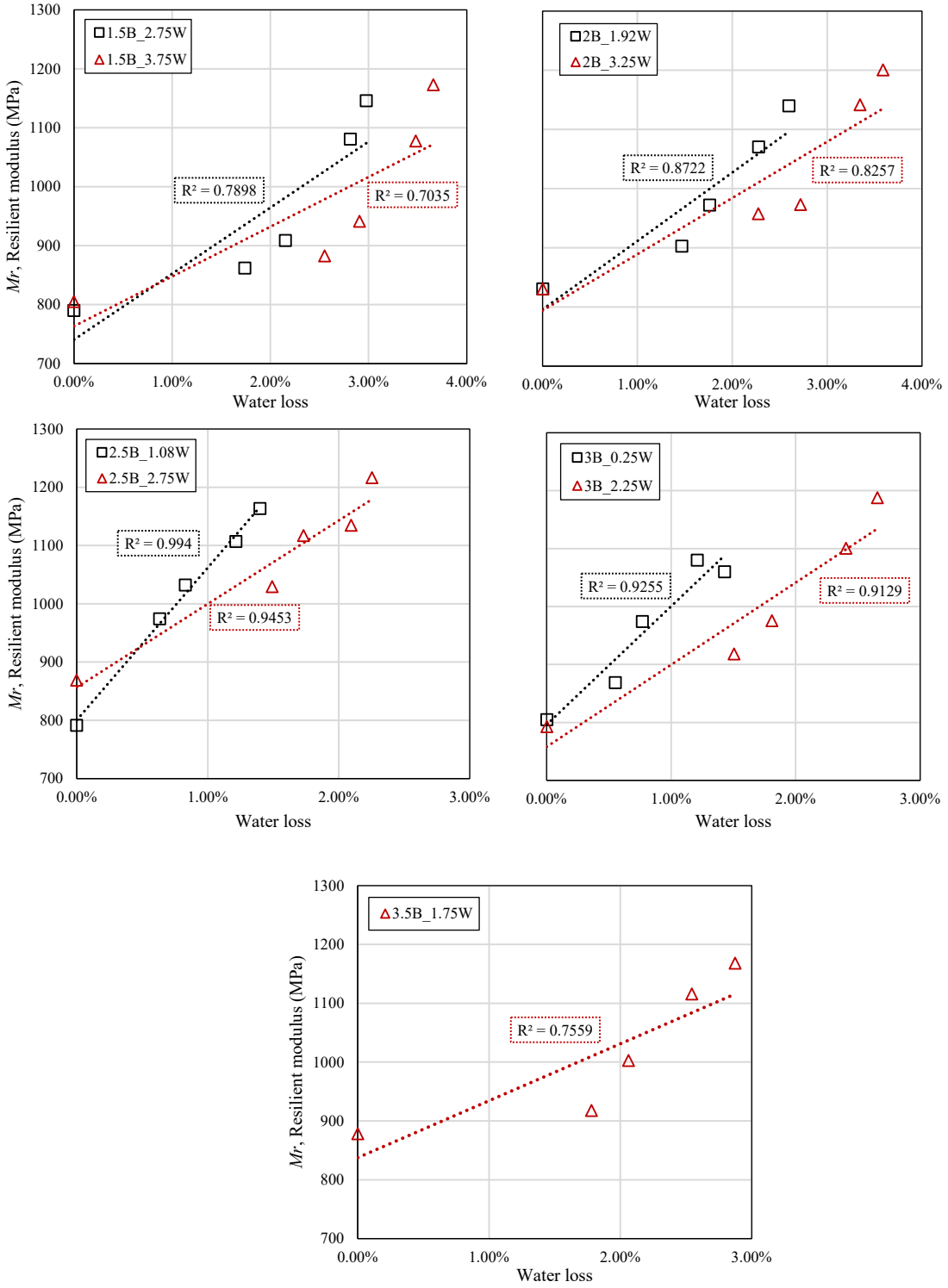

Fig. 6. Correlation between the maximum Mr values (σ_3 = 150 kPa, σ_d = 475 kPa) and the percentage water loss.

However, regarding the *Mr* results at 7 d of the rest of the mixtures with 2.50% BC (without taking into account 2.5B_2.75 W), the difference between the maximum and minimum upper limits of *Mr* ranges reached was reduced to 55.53 MPa (Table 5). The upper limits of the *Mr* ranges reached by mixtures with AWC ranging from 2.00% to 3.00% were again the highest.

Considering more advanced curing times, the graph at 30 d of curing in Fig. 7 showed some stabilization in the maximum *Mr* results, with a difference between maximum and minimum upper limits of *Mr* ranges reached of 56.33 MPa. Despite the small difference and less clear trend, the results obtained by the mixtures with intermediate water contents are still the highest, especially by those with an AWC ranging from 2.00% to 2.75% (Table 5). In the case of the graph at 60 d of curing, mixture 2.5B_3.5 W (the highest AWC studied) exhibited the maximum *Mr* values, despite having one of the worst evolutions and lowest *Mr* values of the mixtures with 2.50% BC in the first week of curing. Again, in view of the graphs in Fig. 6, the *Mr* values achieved in the tests showed to be correlated with the AWC and its evolution with curing

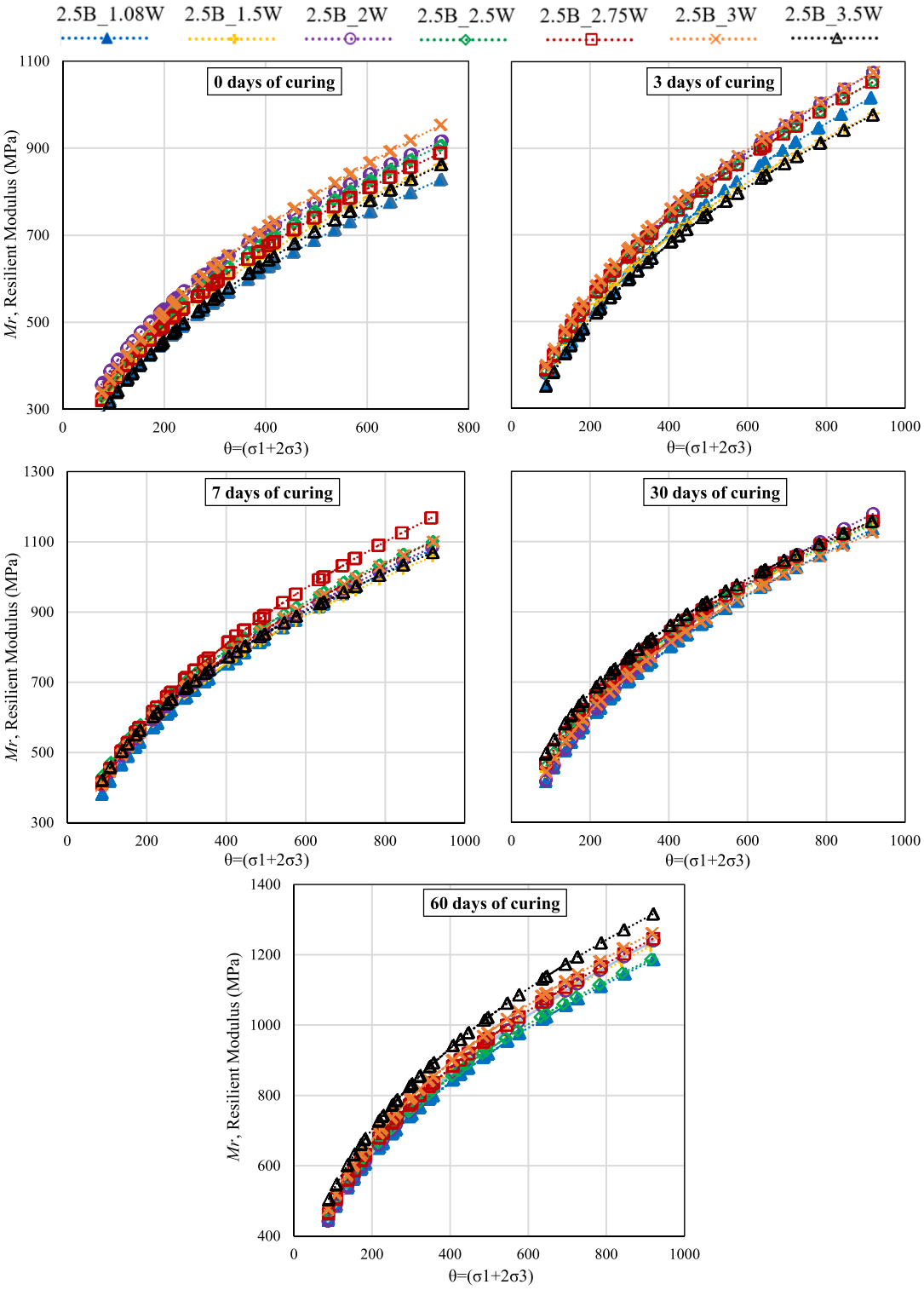

Fig. 7. Representation of the fitted Hicks model for the CIR mixtures with 2.50% BC and different AWC, at 0 d, 3 d, 7 d, 30 d, and 60 d of curing time.

time. The mixture 2.5B_3.5 W used the highest AWC of all those studied, and therefore required a longer curing time to completely develop its stiffness. However, although this mixture obtained the highest *Mr* values after 60 d of curing, its short-term evolution was not good.

Considering the relevance of the short-term behaviour in CIR, it was concluded that for the mixtures using the optimum BC of 2.50%, those with AWC between 2.00% and 2.75% showed the best results. Particularly, mixture 2.5B_2.75 W, designed according to Eq. (2, proved to be the best, with the best short-term evolution and adequate results for more advanced curing.

5.2.2. *Computational modelling of resilient behaviour*

The parameters of the three numerical models were obtained using the Excel optimisation solver, minimising the quadratic error within the predicted models and the actual M_r results from the previously conducted triaxial tests (Table 5). Tables 6, 7, and 8 show the fitted

Table 6
Parameters of Hicks model (k-θ) fitted for CIR mixtures at different curing ages.

	Mixture	1.5B_2.75 W	1.5B_3.75 W	2B_1.92 W	2B_3.25 W	2.5B_1.08 W	2.5B_1.5 W	2.5B_2W	2.5B_2.5 W	2.5B_2.75 W	2.5B_3W	2.5B_3.5 W	3B_0.25 W	3B_2.25 W	3.5B_1.75 W
0 d	k1	43.413	33.947	39.875	27.730	40.592	47.364	59.595	47.148	45.483	43.814	33.907	43.302	42.392	43.500
	k2	0.444	0.486	0.465	0.528	0.456	0.439	0.413	0.447	0.450	0.458	0.481	0.448	0.449	0.455
	R^2	0.947	0.958	0.961	0.949	0.956	0.958	0.958	0.959	0.939	0.959	0.972	0.947	0.954	0.967
3 d	k1	52.416	54.539	44.107	41.642	46.707	58.716	53.312	56.069	57.782	59.758	49.717	53.009	51.432	62.103
	k2	0.415	0.414	0.450	0.467	0.452	0.412	0.440	0.430	0.425	0.424	0.437	0.416	0.430	0.401
	R^2	0.940	0.935	0.954	0.955	0.933	0.950	0.952	0.929	0.920	0.950	0.954	0.938	0.946	0.953
7 d	k1	55.862	54.900	38.617	52.552	53.203	65.660	63.157	72.722	57.108	62.245	69.313	66.341	65.400	71.810
	k2	0.414	0.422	0.480	0.435	0.441	0.407	0.417	0.398	0.443	0.421	0.396	0.399	0.403	0.392
	R^2	0.947	0.951	0.960	0.953	0.946	0.954	0.960	0.948	0.957	0.955	0.952	0.938	0.952	0.947
30 d	k1	63.766	62.384	37.893	57.310	61.809	73.879	58.047	79.886	83.296	75.187	95.959	81.677	84.411	85.783
	k2	0.419	0.423	0.496	0.443	0.427	0.402	0.441	0.391	0.386	0.397	0.361	0.383	0.379	0.379
	R^2	0.961	0.960	0.971	0.969	0.966	0.962	0.964	0.963	0.968	0.955	0.959	0.949	0.963	0.970
60 d	k1	67.591	63.682	46.404	59.549	69.254	71.344	62.937	77.313	70.546	74.839	79.961	61.598	77.358	79.422
	k2	0.419	0.431	0.474	0.444	0.416	0.417	0.437	0.401	0.421	0.414	0.410	0.421	0.406	0.397
	R^2	0.961	0.961	0.974	0.971	0.969	0.961	0.970	0.967	0.969	0.950	0.947	0.970	0.944	0.940

Table 7
Parameters of Uzan model fitted for CIR mixtures at different curing ages.

	Mixture	1.5B_2.75 W	1.5B_3.75 W	2B_1.92 W	2B_3.25 W	2.5B_1.08 W	2.5B_1.5 W	2.5B_2W	2.5B_2.5 W	2.5B_2.75 W	2.5B_3W	2.5B_3.5 W	3B_0.25 W	3B_2.25 W	3.5B_1.75 W
0 d	k1	36.682	28.944	34.190	35.319	34.728	41.208	51.714	40.561	37.785	37.492	29.768	36.639	36.133	38.312
	k2	0.645	0.679	0.649	0.654	0.643	0.615	0.583	0.625	0.670	0.643	0.638	0.647	0.639	0.610
	k3	−0.212	−0.202	−0.194	−0.205	−0.198	−0.188	−0.179	−0.187	−0.232	−0.195	−0.165	−0.209	−0.201	−0.163
	R^2	0.994	0.995	0.997	0.993	0.995	0.996	0.997	0.996	0.994	0.997	0.998	0.993	0.997	0.995
3 d	k1	41.583	44.180	36.405	33.830	35.943	47.922	43.258	42.975	43.824	48.210	40.425	42.091	41.515	51.079
	k2	0.683	0.668	0.682	0.712	0.751	0.652	0.685	0.733	0.735	0.675	0.679	0.681	0.682	0.627
	k3	−0.264	−0.251	−0.230	−0.242	−0.295	−0.237	−0.241	−0.298	−0.304	−0.248	−0.239	−0.260	−0.248	−0.223
	R^2	0.997	0.042	0.991	0.993	0.992	0.996	0.995	0.995	0.990	0.190	0.997	0.992	0.992	0.996
7 d	k1	45.232	44.424	31.594	43.211	42.462	54.043	52.743	59.189	46.808	51.254	57.033	53.050	54.065	58.457
	k2	0.663	0.668	0.723	0.668	0.705	0.633	0.631	0.636	0.676	0.648	0.621	0.660	0.625	0.631
	k3	−0.246	−0.242	−0.242	−0.231	−0.261	−0.222	−0.212	−0.234	−0.231	−0.224	−0.222	−0.257	−0.219	−0.235
	R^2	0.997	0.997	0.996	0.992	0.994	0.995	0.998	0.997	0.995	0.995	0.996	0.996	0.993	0.996
30 d	k1	53.360	52.002	31.710	48.630	52.023	62.270	48.108	67.856	72.266	62.277	81.365	67.022	71.518	74.088
	k2	0.632	0.637	0.706	0.639	0.631	0.601	0.661	0.585	0.554	0.615	0.550	0.613	0.570	0.552
	k3	−0.212	−0.211	−0.208	−0.195	−0.202	−0.197	−0.217	−0.192	−0.167	−0.215	−0.186	−0.226	−0.188	−0.171
	R^2	0.998	0.995	0.998	0.997	0.998	0.997	0.998	0.997	0.994	0.996	0.997	0.997	0.998	0.998
60 d	k1	56.564	52.865	39.415	50.523	59.118	59.680	53.104	66.094	60.133	61.174	64.804	52.352	62.976	69.000
	k2	0.633	0.653	0.670	0.638	0.606	0.629	0.637	0.583	0.611	0.649	0.657	0.613	0.648	0.563
	k3	−0.212	−0.219	−0.194	−0.193	−0.188	−0.210	−0.198	−0.180	−0.188	−0.231	−0.243	−0.190	−0.238	−0.164
	R^2	0.998	0.998	0.998	0.998	0.998	0.998	0.999	0.996	0.998	0.994	0.996	0.999	0.991	0.998

Table 8
Parameters of NCHRP model fitted for CIR mixtures at different curing ages.

	Mixture	1.5B_2.75 W	1.5B_3.75 W	2B_1.92 W	2B_3.25 W	2.5B_1.08 W	2.5B_1.5 W	2.5B_2W	2.5B_2.5 W	2.5B_2.75 W	2.5B_3W	2.5B_3.5 W	3B_0.25 W	3B_2.25 W	3.5B_1.75 W
0 d	k1	3.502	3.315	3.524	3.602	3.447	3.711	4.136	3.830	3.779	3.746	3.201	3.563	3.476	3.644
	k2	0.615	0.652	0.619	0.630	0.617	0.588	0.554	0.597	0.636	0.612	0.609	0.619	0.607	0.578
	k3	−0.558	−0.526	−0.495	−0.548	−0.522	−0.488	−0.457	−0.488	−0.607	−0.496	−0.408	−0.550	−0.516	−0.395
	R^2	0.994	0.995	0.996	0.995	0.995	0.995	0.994	0.995	0.994	0.995	0.995	0.994	0.995	0.991
3 d	k1	3.632	3.756	3.573	3.654	3.842	4.004	4.136	4.170	4.222	4.280	3.785	3.696	3.813	4.008
	k2	0.632	0.626	0.662	0.690	0.716	0.613	0.654	0.691	0.704	0.624	0.641	0.647	0.655	0.593
	k3	−0.497	−0.480	−0.482	−0.503	−0.609	−0.458	−0.486	−0.596	−0.640	−0.453	−0.464	−0.531	−0.510	−0.442
	R^2	0.990	0.117	0.995	0.997	0.995	0.993	0.996	0.994	0.996	0.990	0.994	0.993	0.995	0.994
7 d	k1	3.837	3.909	3.581	3.975	4.145	4.370	4.372	4.642	4.471	4.409	4.387	4.262	4.273	4.464
	k2	0.618	0.623	0.693	0.644	0.669	0.602	0.589	0.597	0.649	0.619	0.589	0.619	0.600	0.596
	k3	−0.466	−0.457	−0.479	−0.478	−0.521	−0.445	−0.393	−0.454	−0.472	−0.449	−0.441	−0.505	−0.451	−0.465
	R^2	0.991	0.992	0.996	0.995	0.994	0.995	0.992	0.993	0.997	0.995	0.995	0.993	0.995	0.995
30 d	k1	4.462	4.453	3.766	4.470	4.475	4.783	4.504	4.913	4.994	4.760	5.131	4.871	4.892	4.973
	k2	0.594	0.608	0.677	0.609	0.593	0.569	0.625	0.546	0.531	0.579	0.513	0.574	0.524	0.518
	k3	−0.401	−0.421	−0.413	−0.378	−0.380	−0.383	−0.416	−0.355	−0.336	−0.419	−0.356	−0.436	−0.334	−0.317
	R^2	0.994	0.995	0.997	0.996	0.994	0.994	0.996	0.992	0.994	0.993	0.991	0.993	0.990	0.994
60 d	k1	4.729	4.720	4.175	4.654	4.768	4.951	4.764	4.959	4.966	5.147	5.406	4.338	5.148	4.994
	k2	0.594	0.612	0.642	0.599	0.566	0.587	0.598	0.545	0.577	0.616	0.614	0.573	0.624	0.525
	k3	−0.401	−0.412	−0.378	−0.357	−0.340	−0.395	−0.364	−0.336	−0.355	−0.462	−0.464	−0.350	−0.498	−0.293
	R^2	0.994	0.993	0.997	0.994	0.993	0.992	0.994	0.991	0.994	0.993	0.991	0.994	0.994	0.993

parameters of the models and the quadratic errors with respect to the experimental values of M_r. These parameters, k_1, k_2, and k_3, are material-specific constants; k_1 is often referred to as the "modulus number"; k_2 is the exponent of bulk stress (θ), indicating the impact on M_r; and k_3 is an exponent that determines the variation rate of M_r with deviatoric stress.

The Hicks model (Table 6) is simpler than the Uzan (Table 7) and NCHRP (Table 8) models, and does not approximate actual M_r values as accurately as the other two models. This is confirmed by the quadratic errors, which were on average 0.9578 for Hicks, and 0.9963 and 0.9939 for Uzan and NCHRP, respectively. The latter methods are much more accurate, as they can accurately approximate the step shape of the experimental M_r results (Fig. 4).

The Hicks model is useful for its simplicity, allowing comparisons such as those in Figs. 5 and 7. However, the resilient modulus of CIR mixtures is not only a function of the sum of the stresses. When the explicit dependence of the deviatoric stress was considered in the model, a decrease in k_1 and an increase in k_2 were observed. This was observed in the Uzan model (Table 7), and even more so in the NCHRP (Table 8). Other studies on cold mixtures have reported this feature [19,21,26]. Another noticeable feature is that parameter k_3 was negative in all cases, indicating the small stress-softening effect due to shear forces overlaid on the macroscopic stress stiffening inherent in the nonlinear elastic behaviour of these mixtures. Other studies have reported that k_3 tended to become very small or even become positive with curing time, which is illogical for the Uzan model [21]. However, although the average value of k_3 slightly decreased with ageing, in all the tested mixtures in this research it remained negative and fairly constant, and no clear trend was observed. Regarding the modulus number, k1, it increased with the curing period, and so did the *Mr* values.

From the uncured results at 0 d, it was not appropriate to derive an optimum binder and water dosages, given the small variation in the results. At this age, the mixtures mainly resist through their internal structure because the binder does not yet provide sufficient cohesion. However, the M_r results for the cured mixtures (Table 5) indicate that the highest values were achieved for 2.50% BC both in the short and long-term. By fixing the BC and varying the water ratio (Fig. 7), it was observed that the highest and the lowest AWC produced worst short-term evolution of M_r. For more advanced curing times, the results at 60 d showed that the mixture with the highest AWC (2.5B_3.5 W) achieved the highest *Mr* values, despite its weak short-term performance. Thus, it was found that mixtures with an AWC around 2.75% (estimated using Eq. (2) from PG-4) had a better short-term evolution of *Mr* and reached adequate values.

As concluded in previous CIR mixture studies [35], the water content was a critical parameter in mix design, and its evolution with the curing of the mixtures had a high linear relationship with the evolution of the stiffness (Fig. 6). Subsequent triaxial testing are showing that *Mr* continued to increase after 60 d of curing, although at a slower rate, and other authors have even reported that the stiffness may continue to increase after longer curing periods [24–26]. Long-term resilient modulus tests to study the evolution of the stiffness may be useful, and will be conducted on the same specimens used in this study.

Generally, all of the studied mixtures exhibited characteristic nonlinear elastic behaviour in terms of stiffness evolution at all curing ages, not only in the short term. The specimens were rather soft at low stresses, with increasing stiffness, especially at greater curing ages with elevated stresses. This behaviour may be especially appropriate for roads with low and medium traffic, allowing adaptation to deflections with no cracks or brittleness at low loading moments (which are frequent on such roads) and providing adequate resistance when higher loads are applied.

6. Conclusions

In this study, the resilient moduli (M_r) of different CIR mixtures at

different curing ages were obtained experimentally to better understand the mechanical behaviour of these mixtures in the short term and their evolution with curing time. Three behavioural prediction models were matched to the obtained results. The adjusted model values can be used in subsequent research to perform mathematical simulations of the behaviour of CIR mixtures. The following are the conclusions of this study.

1. The dynamic triaxial tests performed on CIR mixtures indicated a significant dependence on the principal stresses σ_1 and σ_3, highlighting their nonlinear elastic nature. The resilient modulus variation was found to be greater with confining stress (σ_3) than with deviatoric stress (σ_d).
2. The Uzan and NCHRP models were found to be more accurate in terms of numerical modelling of the resilient behaviour of the CIR mixtures, fitting better to the experimental results. However, the Hicks model, owing to its simplicity, was useful for comparison of the nonlinear elastic behaviour between different CIR mixtures.
3. It was observed that the increase in the stiffness in different mixes followed a growth rate analogous to that of the water loss with curing. During the first days of curing (from 0 d to 7 d), when there was a greater evaporation of water from the mixtures, the greatest increase in the M_r ranges was observed; after 7d, and especially between 30 d and 60 d, when water loss stabilized, the increase in M_r was slower.
4. Dynamic triaxial tests performed at 0 d of curing showed similar behaviour between mixtures, highlighting the minor influence of the binder at this stage, mainly owing to its mineral skeleton.
5. Dynamic triaxial tests conducted on specimens during the first days of curing, at 3 d and at 7d, showed a greater variation in the evolution of stiffness, allowing the identification of binder and added water contents that provided the best performance. After 30 d and 60 d of curing, the evolution was slower.
6. Mixtures with 2.50% BC produced the highest resilient moduli and the best evolution with curing time of all mixtures manufactured according to PG-4.
7. The AWC of the mixtures and its evolution with curing time (by evaporation) were correlated with the maximum *Mr* values reached. This relationship resulted to be rather linear for the mixes with BC between 2.00% and 3.00%.
8. By fixing BC at 2.50% and varying the AWC, the mixtures with 2.00% to 2.75% AWC showed the best evolution in the results. In particular, the mixture with 2.50% BC and 2.75% AWC was the one that presented the best short-term development of *Mr* and reached adequate values.

All of the mixtures presented characteristic nonlinear elastic behaviour at all curing ages. They were rather soft at low stresses, with a significant increase in stiffness at high stresses. This behaviour could be especially appropriate for roads with low to medium traffic, allowing adaptation to deformations with no cracking when loads are low and providing adequate resistance when higher loads are applied.

Declaration of Competing Interest

The authors declare that they have no known competing financial interests or personal relationships that could have appeared to influence the work reported in this paper.

Acknowledgements

The authors would like to acknowledge funding for the project BIA2016-80317-R/AEI/10.13039/501100011033 from the Spanish Ministry of Science and Innovation, with an associated pre-doctoral scholarship for the training of research workers (FPI) BES-2017-079633. The authors would also like to express their sincere gratitude to ARIAS INFRAESTRUCTURAS, and ECOASFALT for their generous donation of RAP and bitumen emulsions, respectively, for this research. The funding of the open access charge was made by Universidade da Coruña/CISUG.

References

[1] F. Xiao, S. Yao, J. Wang, X. Li, S. Amirkhanian, A literature review on cold recycling technology of asphalt pavement, Constr. Build. Mater. 180 (2018) 579–604, https://doi.org/10.1016/j.conbuildmat.2018.06.006.
[2] J. Zhu, T. Ma, Z. Dong, Evaluation of optimum mixing conditions for rubberized asphalt mixture containing reclaimed asphalt pavement, Constr. Build. Mater. 234 (2020) 117426, https://doi.org/10.1016/j.conbuildmat.2019.117426.
[3] T. Wang, F. Xiao, X. Zhu, B. Huang, J. Wang, S. Amirkhanian, Energy consumption and environmental impact of rubberized asphalt pavement, J. Cleaner Prod. 180 (2018) 139–158, https://doi.org/10.1016/j.jclepro.2018.01.086.
[4] N. Thom, A. Dawson, Sustainable Road Design: Promoting Recycling and Non-Conventional Materials, Sustainability 11 (21) (2019) 6106, https://doi.org/10.3390/su11216106.
[5] F. Gu, W. Ma, R.C. West, A.J. Taylor, Y. Zhang, Structural performance and sustainability assessment of cold central-plant and in-place recycled asphalt pavements: a case study, J. Cleaner Prod. 208 (2019) 1513–1523, https://doi.org/10.1016/j.jclepro.2018.10.222.
[6] G. Valdes-Vidal, A. Calabi-Floody, E. Sanchez-Alonso, Performance evaluation of warm mix asphalt involving natural zeolite and reclaimed asphalt pavement (RAP) for sustainable pavement construction, Constr. Build. Mater. 174 (2018) 576–585, https://doi.org/10.1016/j.conbuildmat.2018.04.149.
[7] A. Nättorp, F. Dinkel, M. Zschokke, Environmental impact of biogenic oils as raw materials in road construction, Int. J. Pavement Eng. 20 (6) (2019) 714–723, https://doi.org/10.1080/10298436.2017.1330080.
[8] A. Pakes, T. Edil, M. Sanger, R. Olley, T. Klink, Environmental benefits of cold-in-place recycling, Transp. Res. Rec. 2672 (24) (2018) 11–19, https://doi.org/10.1177/0361198118758691.
[9] Salomon, A., & Newcomb, D. E. (2000). Cold in-place recycling literature review and preliminary mixture design procedure.
[10] E. Garilli, F. Autelitano, C. Godenzoni, A. Graziani, F. Giuliani, Early age evolution of rheological properties of over-stabilized bitumen emulsion-cement pastes, Constr. Build. Mater. 125 (2016) 352–360, https://doi.org/10.1016/j.conbuildmat.2016.08.054.
[11] Y. Niazi, M. Jalili, Effect of Portland cement and lime additives on properties of cold in-place recycled mixtures with asphalt emulsion, Constr. Build. Mater. 23 (3) (2009) 1338–1343, https://doi.org/10.1016/j.conbuildmat.2008.07.020.
[12] A. Behnood, M.M. Gharehveran, F.G. Asl, M. Ameri, Effects of copper slag and recycled concrete aggregate on the properties of CIR mixes with bitumen emulsion, rice husk ash, Portland cement and fly ash, Constr. Build. Mater. 96 (2015) 172–180, https://doi.org/10.1016/j.conbuildmat.2015.08.021.
[13] J. Lin, L. Huo, F. Xu, Y. Xiao, J. Hong, Development of microstructure and early-stage strength for 100% cold recycled asphalt mixture treated with emulsion and cement, Constr. Build. Mater. 189 (2018) 924–933, https://doi.org/10.1016/j.conbuildmat.2018.09.064.
[14] S. Raschia, C. Mignini, A. Graziani, A. Carter, D. Perraton, M. Vaillancourt, Effect of gradation on volumetric and mechanical properties of cold recycled mixtures (CRM), Road Materials and Pavement Design 20 (sup2) (2019) S740–S754, https://doi.org/10.1080/14680629.2019.1633754.
[15] A. Graziani, C. Iafelice, S. Raschia, D. Perraton, A. Carter, A procedure for characterizing the curing process of cold recycled bitumen emulsion mixtures, Constr. Build. Mater. 173 (2018) 754–762, https://doi.org/10.1016/j.conbuildmat.2018.04.091.
[16] Wirtgen Group. Wirtgen Cold Recycling Technology, 1st ed.; Wirtgen GmbH: Windhagen, Germany, 2012; pp. 18–19.
[17] Southern African Bitumen Association (Sabita). A Guideline for the Design and Construction of Bitumen Emulsion and Foamed Bitumen Stabilised Materials; Technical Guideline: Bitumen Stabilised Materials, 3rd ed.; Southern African Bitumen Association (Sabita): Cape Town, South Africa, 2020; pp. 1–2, 7–8, 36–37.
[18] K.J. Jenkins, F.M. Long, L.J. Ebels, Foamed bitumen mixes= shear performance? Int. J. Pavement Eng. 8 (2) (2007) 85–98, https://doi.org/10.1080/10298430601149718.
[19] L.J. Ebels, Characterisation of material properties and behaviour of cold bituminous mixtures for road pavements (Doctoral dissertation, Stellenbosch University), Stellenbosch, 2008.
[20] F. Lekarp, U. Isacsson, A. Dawson, State of the art. I: Resilient response of unbound aggregates, J. Transp. Eng. 126 (1) (2000) 66–75, https://doi.org/10.1061/(ASCE)0733-947X(2000)126:1(66).
[21] E. Santagata, G. Chiappinelli, P.P. Riviera, O. Baglieri, Triaxial testing for the short term evaluation of cold-recycled bituminous mixtures, Road Mater. Pav. Des. 11 (1) (2010) 123–147, https://doi.org/10.1080/14680629.2010.9690263.
[22] W. Fedrigo, W.P. Núñez, M.A.C. López, T.R. Kleinert, J.A.P. Ceratti, A study on the resilient modulus of cement-treated mixtures of RAP and aggregates using indirect tensile, triaxial and flexural tests, Constr. Build. Mater. 171 (2018) 161–169, https://doi.org/10.1016/j.conbuildmat.2018.03.119.
[23] S. Casillas, A. Braham, Quantifying effects of laboratory curing conditions on workability, compactability, and cohesion gain of cold in-place recycling, Road Materials and Pavement Design 22 (10) (2021) 2329–2351, https://doi.org/10.1080/14680629.2020.1753101.

[24] B. Dolzycki, M. Jaczewski, C. Szydlowski, The long-term properties of mineral-cement-emulsion mixtures, Constr. Build. Mater. 156 (2017) 799–808, https://doi.org/10.1016/j.conbuildmat.2017.09.032.
[25] A. Graziani, C. Godenzoni, F. Cardone, M. Bocci, Effect of curing on the physical and mechanical properties of cold-recycled bituminous mixtures, Mater. Des. 95 (2016) 358–369, https://doi.org/10.1016/j.matdes.2016.01.094.
[26] A.K. Kuchiishi, C.C.D.S. Antão, K. Vasconcelos, J. Pires, O.M.D.O. Araújo, L.L. B. Bernucci, R.T. Lopes, Investigation of the matric suction role on the curing mechanism of foamed asphalt stabilised mixtures, Road Materials and Pavement Design 20 (sup1) (2019) S365–S389, https://doi.org/10.1080/14680629.2019.1589558.
[27] A.K. Kuchiishi, K. Vasconcelos, L.L. Bariani Bernucci, Effect of mixture composition on the mechanical behaviour of cold recycled asphalt mixtures, Int. J. Pavement Eng. 22 (8) (2021) 984–994, https://doi.org/10.1080/10298436.2019.1655564.
[28] B. Gómez-Meijide, I. Pérez, Nonlinear elastic behavior of bitumen emulsion-stabilized materials with C&D waste aggregates, Constr. Build. Mater. 98 (2015) 853–863, https://doi.org/10.1016/j.conbuildmat.2015.07.004.
[29] L.J. Ebels K.J. Jenkins Determination of material properties of bitumen stabilised materials using tri-axial testing 2006 QUEBEC CITY, CANADA.
[30] Ministry of Development (2017) Recycling of bituminous pavements and roadways. Circular Order 40/2017. *In Spanish.*
[31] AENOR, Spanish, Tests to determine the mechanical and physical properties of aggregates. Part 6: Determination of particle density and water absorption, Association for Standardisation and Certification, Madrid, Spain. In Spanish, 2006.
[32] NLT standards. NLT-164/90. Binder content in bituminous mixtures. Road tests Directorate General for Roads 2nd ed. 1990 Ministry of Public Works and Transport Madrid, Spain. In Spanish.
[33] AENOR, Spanish Association for Standardisation and Certification UNE-EN 1426 2015 Bitumen and bituminous binders. Determination of needle penetration Madrid, Spain In Spanish.
[34] AENOR, Spanish Bitumen and bituminous binders. Determination of the softening point 2015 Association for Standardisation and Certification Madrid, Spain. In Spanish.
[35] P. Orosa, A.R. Pasandín, I. Pérez, Assessment of two laboratory design methods for CIR mixtures with bitumen emulsion based on static and gyratory compaction, Constr. Build. Mater. 265 (2020) 120667, https://doi.org/10.1016/j.conbuildmat.2020.120667.
[36] P. Orosa, A.R. Pasandín, I. Pérez, Compaction and volumetric analysis of cold in-place recycled asphalt mixtures prepared using gyratory, static, and impact procedures, Constr. Build. Mater. 296 (2021) 123620, https://doi.org/10.1016/j.conbuildmat.2021.123620.
[37] AENOR, Spanish Association for Standardization and Certification, 2013. UNE-EN 13808:2013. Bitumen and bituminous binders - Framework for specifying cationic bituminous emulsions. Madrid, Spain, 2013. *In Spanish.*
[38] Ministry of Development (2001) "Pavement recycling". Circular Order 8/2001. *In Spanish.*
[39] M. Piratheepan, (2011). Designing Cold Mix Asphalt (CMA) and Cold-In-Place Recycling (CIR) Using Superpave Gyratory Compactor (Doctoral dissertation).
[40] AENOR, Spanish In Spanish UNE-EN 12697–31. Bituminous mixtures. Test methods for hot bituminous mixtures. Part 31: Specimen preparation by gyratory compactor. Madrid 2008 Association for Standardization and Certification.
[41] AENOR, Spanish Association for Standardization and Certification, 2008. UNE-EN 13286-7:2008. Unbound and hydraulically bound mixtures - Part 7: Cyclic load triaxial test for unbound mixtures. Madrid, Spain, 2008. *In Spanish.*
[42] T. Yun, Y.R. Kim, Viscoelastoplastic modeling of the behavior of hot mix asphalt in compression, KSCE J. Civ. Eng. 17 (6) (2013) 1323–1332, https://doi.org/10.1007/s12205-013-0352-7.
[43] W. Kim, J. Labuz, Resilient modulus and strength of base course with recycled bituminous material, (Technical report) (2007).
[44] Brown, S. F., & Pell, P. S. (1967, January). An experimental investigation of the stresses, strains and deflections in a layered pavement structure subjected to dynamic loads. In *Intl Conf Struct Design Asphalt Pvmts*.
[45] Hicks, R. G., & Monismith, C. L. (1972, September). Prediction of the resilient response of pavements containing granular layers using Non-linear Elastic Theory. In *Presented at the Third International Conference on the Structural Design of Asphalt Pavements, Grosvenor House, Park Lane, London, England, Sept. 11-15, 1972.* (Vol. 1, No. Proceeding).
[46] R.G. Hicks, Factors influencing the resilient response of granular materials (Doctoral dissertation), University of California, Berkeley, USA), 1970.
[47] J. Uzan M.W. Witczak T. Scullion R.L. Lytton Development and validation of realistic pavement response models 1992 Nottingham, UK.
[48] NCHRP, (National Cooperative Highway Research Program), Guide for Mechanistic-Empirical Design of New and Rehabilitated Pavement Structures. Part 2. Design Inputs, Final Report NCHRP (2004) 1–37A.
[49] D. Andrei, Development of a harmonized test protocol for the resilient modulus of unbound materials used in pavement design (Doctoral dissertation, University of Maryland, College Park), 1999.
[50] A.H.M.D. Silva, Avaliação do comportamento de pavimentos com camada reciclada de revestimentos asfálticos a frio com emulsão modificada por polímero (Doctoral dissertation, Universidade de São Paulo), 2011.
[51] L.R.D. Andrade, Comparação do comportamento de pavimentos asfálticos com camadas de base granular, tratada com cimento e com estabilizantes asfálticos para tráfego muito pesado (Doctoral dissertation, Universidade de São Paulo), 2016.